

Evaluation of the Changes Created by Endosteal Implants Installed at Different Lengths, Angles and Diameters on the Maxilla and Mandible Using Three-Dimensional Modeling and Finite Elements Stress Analysis

Nedim Güneş^{1*}, Rezzan Güner²

1. Dicle University, Faculty of Dentistry, Department of Oral and Maxillofacial Surgery, Diyarbakir, Turkey.
2. Private Clinic, 31070 Antakya, Turkey.

Abstract

The aim of this study was to compare the stress values on the implant caused by the change in the implant diameter, length, and the angle of the implant placement. Thus, our goal was to determine the correct implant preference with regard to the appropriate diameter, length, and insertion angle.

In our study, a total of 6 different types of implants with 2 different diameters (3.7 mm and 4.7 mm) and 3 different lengths (5 mm, 10mm, and 13mm) belonging to these diameters were selected. These 6 different sized dental implants were applied to the maxilla and mandible, vertically and angled, and a total of 24 models were obtained. The maximum and minimum principal stress values in cortical and cancellous bone were determined as a result of the applied forces.

The maximum and minimum von mises stress values and the places where they occurred were determined as a result of the application of the vertical and oblique (30 °) forces, with a total of 300 N from the 3 different occlusal points by placing Zimmer brand implants that were 5, 10, and 13 mm in length and 3.7 and 4.7 mm in diameter on the maxilla and mandible separately at an angle of 30 °.

Taken together, in all models, under each loading condition, as the implant diameter and length increased, the stress levels in the bone and implant decreased. Thus, implant diameter is more effective than implant length at changing the stress values. There was a significant increase in the stress levels of the cortical bone and implants in the oblique loading models compared to the vertical loading models.

Experimental article (J Int Dent Med Res 2021; 14(2): 505-513)

Keywords: Finite elements methods, dental implants, biomechanics, stress distribution.

Received date: 01 February 2021

Accept date: 24 March 2021

Introduction

In the general literature, materials that replace a missing organ or tissue are defined as implants. In the dental field, biocompatible, biofunctional materials that are placed in or on the bone to support the restoration of a lost tooth and the surrounding tissues are defined as implants.¹ Numerous published clinical studies on dental implant procedures report an approximately 99 % long-term osteointegration rate. Therefore, the use of implants in the oral

field has become more and more effective.²

The periodontal ligament acts as a shock absorber in natural teeth. In osseointegrated dental implants, occlusal loads are transmitted directly to the bone depending on the movement. This situation may cause microfractures at the bone and implant interface, fractures in the implant, the loss of implant components, and bone loss. In this regard, it is very important to analyze the various stress distributions around the implants. These stress distributions are affected by the thread geometry, thread depth, thread pitch, implant length, implant diameter, implant neck design, and implant placement angle.³

The success rate of dental implants depends on the quality of the jawbone, the implant design, the surface structure of the implant, and the surgical procedures. With regard to implant design, the implant diameter and

*Corresponding author:

Nedim Güneş
Dicle University, Faculty of Dentistry,
Department of Oral and Maxillofacial Surgery,
Diyarbakir, Turkey.
E-mail: nedimgunes1905@hotmail.com

length directly affect the primary stability, placement, and extractor torque values of the implant. Many studies have been conducted to assess these characteristics, revealing that these are the main factors related to implant success.⁴ The concept of "osseointegration" was proposed by Branemark et al. and forms the basis of implant success. During the osseointegration of endosseous dental implants, the amount of bone alone is not the determining criterion for success. The bone should also have sufficient density. The density of the bone in the toothless area is effective in the treatment planning, implant design, surgical approach, healing process, and when deciding on the loading process of the prosthesis.⁵

Biomechanical factors are very important in the long-term success of dental implants.^{6,7} Occlusal loads are transmitted to dental implants and the surrounding bone via prosthesis over implants. Loads transmitted on the implants cause stresses at the implant-bone interface depending on the type of load, the dimensions of the implants, the surface properties of the implants, the type of prosthesis, the structural features of the bone around the implants, and the placement of the implants. Excessive loads that exceed the bearing capacity of the bone at the implant-bone interface may affect bone remodeling and cause resorption and the loss of the implant in more advanced cases.^{8,9}

"Finite Element Stress Analysis" (FESA) has been used in oral implantology since 1976 to measure the changes due to the application of force in the contact area of the implant and bone.^{10,11} FESA is the realization of analyzes by dividing an object with a complex geometry, which is desired to be examined in terms of biomechanics, into a certain number of elements.^{12,13} Since bone, the implant, and supra-implant structures can be modeled close to clinical conditions with FESA analysis, it is possible to precisely determine the amount and localization of the stress, deformation, and displacement in the implants and the surrounding bone under the applied forces.^{14,15,16}

The aim of this study was to compare the stress values on the implant caused by the change in the implant diameter, length, and the angle of the implant placement. Thus, our goal was to determine the correct implant preference with regard to the appropriate diameter, length, and insertion angle.

Materials and methods

This research was carried out in Dicle University Faculty of Dentistry and Dicle University Faculty of Engineering and Architecture. In our study, a total of 6 different types of implants with 2 different diameters (3.7 mm and 4.7 mm) and 3 different lengths (5 mm, 10mm, and 13mm) belonging to these diameters were selected. These 6 different sized dental implants were applied to the maxilla and mandible, vertically and angled, and a total of 24 models were obtained. The abutment and metal-supported ceramic crowns were transferred to all the implants with a Next Engine (Next Engine, Inc.401 Wilshire Blvd., Ninth Flor Santa Monica, CA 90401) 3D laser scanner and the Rhinoceros 4.0 (3670 Woodland Park Ave N, Seattle, WA 98103 USA) software program. A total of 48 study groups were obtained by applying forces separately in the vertical and oblique directions from certain points of the metal supported ceramic crowns. The maximum and minimum principal stress values in cortical and cancellous bone were determined as a result of the applied forces. In addition, the 3-dimensional (3D) finite element stress analysis method (FESA) was used to determine the Von mises stress values in the implants.

In order to make the 3D network topology more homogenous and arrange it, to design the 3D solid model, and also for the FESA, a computer with an Intel Pentium® D CPU 3,00 GHz, 250-GB hard disk, 300-GB RAM and Windows XP Professional Version 2002 Service Pack 3 was used. The 3D scanning was done with macro resolution by means of a Next Engine (Next Engine, Inc. 401 Wilshire Blvd., Ninth Flor Santa Monica, CA 90401) laser scanner, and the 3D modeling software Rhinoceros 4.0 (3670 Woodland Park Ave N, Seattle, WA 98103 USA) and ANSYS (analysis program) were used.

Cortical and Spongy Bone Modeling

The Rhinoceros 4.0 software was used for cortical and cancellous bone modeling. This software, which is capable of 3D modeling, is generally used in industrial design, architecture, boat design, jewelry design, automotive design, CAD/CAM, rapid prototype manufacturing, reverse engineering, and multimedia design. This software obtains images by many imaging methods, including magnetic resonance and computer tomography, that can be reconstructed

in a computer environment. With the software, changes, such as simplification and reformatting, can be made on the reconstructed images. With the mesh simplification tools in this software, models with low memory consumption and uniform proportions can be made. First, the upper jaw and mandible bones of 30 mm x 20 mm x 10 mm were modeled. In the model, we utilized cortical bone that was formed with a thickness of 2 mm in the mandible and 1 mm in the maxilla. The cortical bone inner surface was defined as cancellous bone.

Implant and Abutment Modeling

Six different sized implants and abutments from the Zimmer company were used in the study. The implants were 3.7 mm and 4.7 mm in diameter and 5 mm, 10 mm, and 13 mm in length. These 6 implants and abutments were 3D scanned in the Next Engine 3D laser scanner in macro mode. The Next Engine laser scanner scans physical objects and transfers them to a virtual environment in 3D. With the Scan Studio Core program provided with the device, operations such as scanning, cleaning, alignment, and merging, were performed, and the 3D data obtained was output in stl, obj, vrml, and ucd formats. The point clouds obtained from the scanning implants and abutments were saved in stl. format. Files in this format were transferred to the Rhinoceros 4.0 software. The 6 different implants were placed perpendicular and angled in the middle of the obtained mandible and maxilla bone models as closely as possible. The implants were considered 100 % osseointegrated into the bone.

Coping and Crown Modeling

The crown model was obtained by collecting the tooth sizes and images taken from the Wheeler Dental Anatomy Atlas and transferring these to the Rhinoceros 4.0 software, and the coping was obtained by matching it with the abutment underneath.

Metal-supported porcelain restorations were selected as an over-implant prosthesis type. Chrome-cobalt alloy (Wiron 99; Bego, Bremen, Germany) was used as the substructure, and feldspathic porcelain (Ceramco II; Dentsply, Burlington, USA) was used as the superstructure. While the coping thickness was 0.8 mm, the porcelain thickness was prepared at a minimum of 2 mm considering the crown dimensions. The compatibility of the metal-supported ceramic restoration obtained with the abutment was made

using Rhinoceros 4.0 software.

The models made in Rhinoceros 4.0 were transferred to ANSYS software in stl. format by keeping 3D coordinates. Here, the models were converted to solid models in the form of bricks and tetrahedra elements. In the bricks and tetrahedra solid modeling system, 8-node elements (brick type) were used as much as the ANSYS software could create in the model. In the areas close to the center of the structures in the models, 7-node, 6-node, 5-node, and 4-node elements were used to complete the structure when necessary. Thanks to this modeling technique, we created the highest quality network structure with the highest possible node elements in order to facilitate the calculation. The vertical and narrow areas in the jaw models, which made the analysis process difficult, were made regular by removing the linear elements. Because the coordinate information of the nodes was stored in stl. format, there was no information loss when transferring between the programs.

Modeling the structures

A 1 mm cortical bone around the maxilla and a cancellous bone with a D4 feature below it was modeled. Around the mandible, 2 mm of cortical bone and a dense trabecular bone with a D2 feature below it was modeled. The dental implant and abutment made of titanium were scanned and modeled in the Next Engine laser scanner, and the model was transferred to the computer environment with the Rhinoceros 4.0 software program.

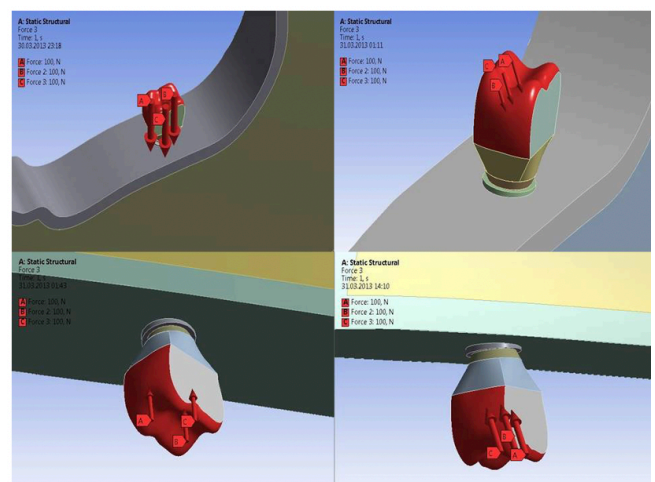


Figure 1. The vertical and angled forces applied to the mandible and maxilla models and their quantities.

Chromium-cobalt alloy was placed on the abutment as a metal substructure. Feldspathic porcelain was placed on the metal substructure. A connection was established between the abutment and superstructure using polycarboxylate cement. The dental implant was made of titanium, chromium-cobalt alloy, feldspathic porcelain, and polycarboxylate cement, and Young's modulus (elasticity modulus) and Poisson ratios of the cortical and cancellous bone were determined. The Young's modulus and Poisson ratio were selected according to the materials, and these materials were transferred to the computer environment. The computer implants were placed in the lower jaw and upper jaw in the first molar area. When the lower jaw was in the first molar centric occlusion, 100 N of force, which was 300 N in total, was simultaneously applied to the buccal tubercle, mesial fossa, and distal fossa regions. When the upper jaw was in centric occlusion in the first molar region, a force of 100 N was applied to the palatal tubercle, mesial fossa, and distal fossa regions at the same time. Thus, a total of 300 N of force was applied to the 48 prepared working models as explained one by one (Figure 1).

Results

		VERTICAL FORCE			OBLIQUE FORCE		
		5 mm length	10 mm length	13 mm length	5 mm length	10 mm length	13 mm length
VERTICAL IMPLANT	3.7 mm diameter	122,22	86,21	84,88	302,37	280,72	253,88
	4.7 mm diameter	87,94	83,88	74,08	146,59	130,32	124,33
		VERTICAL FORCE			OBLIQUE FORCE		
		5 mm length	10 mm length	13 mm length	5 mm length	10 mm length	13 mm length
ANGULAR IMPLANT	3.7 mm diameter	86,71	95,90	92,78	300,69	311,59	317,35
	4.7 mm diameter	70,45	72,30	82,79	190,34	199,41	235,74

Table 1. Von misses stress values (in MPa) occurred in maxilla and implant.

The maximum and minimum von misses stress values and the places where they occurred were determined as a result of the application of the vertical and oblique (30 °) forces, with a total of 300 N from the 3 different occlusal points by placing Zimmer brand implants that were 5, 10, and 13 mm in length and 3.7 and 4.7 mm in diameter on the maxilla and mandible separately at an angle of 30 °. The stress values determined in the maxilla and mandible are presented (Table 1 and Table 2).

Von misses stress values released as a result of the vertical and oblique force applied on the implants placed in the maxilla.

		VERTICAL FORCE			OBLIQUE FORCE		
		5 mm length	10 mm length	13 mm length	5 mm length	10 mm length	13 mm length
VERTICAL IMPLANT	3.7 mm diameter	66,25	62,51	59,40	287,82	244,52	294,38
	4.7 mm diameter	41,66	36,34	31,21	137,61	120,68	120,65
		VERTICAL FORCE			OBLIQUE FORCE		
		5 mm length	10 mm length	13 mm length	5 mm length	10 mm length	13 mm length
ANGULAR IMPLANT	3.7 mm diameter	76,24	74,62	67,85	355,20	336,60	297,41
	4.7 mm diameter	48,99	43,14	46,24	202,69	182,36	202,91

Table 2. Von misses stress values (in MPa) occurred in mandible and implant.

According to the stress analysis obtained from the implants with a length of 5 mm and a diameter of 3.7 mm, the maximum stress occurred at the apical region of the implant when the implant placed at a right angle and in the models with a vertical force, and the minimum stress occurred at the apical 1/3. The maximum stress occurred in the neck of the implant when the implant was placed at a right angle and the models applied force in the oblique direction, and the minimum stress occurred at the apical area. In the implant placed at an angle of 30° and in

the models with a vertical force, the maximum stress occurred in the neck of the implant, and the minimum stress occurred at the apical 1/3. The maximum stress occurred at the implant-abutment junction when the implant was placed at an angle of 30° and in the models where the applied force was in the oblique direction, and the minimum stress occurred at the apical 1/3.

According to the stress analysis obtained from the implants with a length of 5 mm and a diameter of 4.7 mm, the maximum stress occurred at the apical region of the implant when the implant was placed at a right angle and the models used a vertical force, and the minimum stress occurred at the apical 1/3. The maximum stress occurred in the neck of the implant when the implant was placed at a right angle and the models applied force in the oblique direction, and it the minimum stress occurred at the apical region. When the implant was placed at an angle of 30° and the models used vertical force, the maximum stress occurred in the neck of the implant, and the minimum stress occurred just below the implant neck area. The maximum stress occurred at the implant-abutment junction when the implant was placed at an angle of 30° and the models applied the force in the oblique direction, and the minimum stress occurred at the apical 1/3.

According to the stress analysis obtained from the implants with a length of 10 mm and a diameter of 3.7 mm, the maximum stress occurred at the apical region of the implant when the implant placed at a right angle and the models used a vertical force, and the minimum stress occurred in the neck area. The maximum stress occurred in the neck of the implant when the implant was placed at a right angle and the models applied a force in the oblique direction, and the minimum stress occurred at apical 1/2. The maximum stress occurred in the neck of the implant when the implant was placed at an angle of 30° and the models used a vertical force, and the minimum stress occurred at the apical 1/3. The maximum stress occurred at the implant-abutment junction when the implant was placed at an angle of 30° and the models applied a force in the oblique direction, and the minimum stress occurred just below the neck area.

According to the stress analysis obtained from the implants with a length of 10 mm and a diameter of 4.7 mm; the maximum stress occurred at the apical region of the implant when

the implant was placed at a right angle and the models used a vertical force, and the minimum stress occurred in the neck area. The maximum stress occurred in the neck of the implant when the implant was placed at a right angle and the models applied a force in the oblique direction, and the minimum stress occurred at the apical 1/3. The maximum stress occurred in the neck of the implant when the implant was placed at an angle of 30° and the models used a vertical force, and the minimum stress occurred just below the neck area. The maximum stress occurred in the neck area when the implant was placed at an angle of 30° and the models applied a force in the oblique direction, and minimal stress was detected at the apical region.

According to the stress analysis obtained from implants with a length of 13 mm and a diameter of 3.7 mm, the maximum stress occurred at the apical region of the implant when the implant was placed at a right angle and the models used a vertical force, and the minimum stress occurred in the neck area. The maximum stress occurred in the neck of the implant when the implant was placed at a right angle and the models applied a force in the oblique direction, and the minimum stress occurred at the apical region. The maximum stress was observed in the neck of the implant when the implant was placed at an angle of 30° and the models used a vertical force and the minimum stress occurred in the apical 1/3 of the implant. The maximum stress occurred between the neck region and the abutment when the implant was placed at an angle of 30° and the models applied a force in the oblique direction, and the minimum stress occurred in 1/2 of the apical region.

According to the stress analysis obtained from 13 mm long and 4.7 mm diameter implants, the maximum stress occurred at the apical region of the implant when the implant was placed at a right angle and the models used a vertical force, and the minimum stress occurred in the neck area. The maximum stress occurred in the neck of the implant when the implant was placed at a right angle and the models applied a force in the oblique direction, and the minimum stress occurred at the apical region of the implant. The maximum stress was observed in the apical region of the implant when the implant was placed at an angle of 30° and the models used a vertical force, and the minimum stress occurred just below the neck of the implant. The maximum

stress occurred in the neck of the implant when the implant was placed at an angle of 30° and the models applied a force in the oblique direction, and the minimum stress occurred in 1/2 of the apical region.

Von misses stress values resulting from the vertical and oblique force applied on the implants placed in the mandible

According to the stress analysis obtained from the implants with a length of 5 mm and a diameter of 3.7 mm, the maximum stress occurred in the neck of the implant when the implant was placed at a right angle and the models used a vertical force, and the minimum stress occurred in the apical region of the implant. The maximum stress occurred in the neck of the implant when the implant was placed at a right angle and the models applied a force in the oblique direction, and the minimum stress occurred in the apical 1/3 region of the implant. The maximum stress was observed at the junction of the implant abutment when the implant was placed at an angle of 30° and the models used a vertical force, and the minimum stress occurred in the apical 1/3 region of the implant. The maximum stress occurred between the implant and the abutment when the implant was placed at an angle of 30° and the models applied a force in the oblique direction, and minimal stress occurred at the apical region. The maximum stress occurred in the neck of the implant when the implant was placed at a right angle and the models used a vertical force, and the minimum stress occurred in the apical region of the implant. The maximum stress occurred in the neck of the implant when the implant was placed at a right angle and the models applied a force in the oblique direction, and the minimum stress occurred in the apical 1/3 region of the implant.

According to the stress analysis obtained from the implants with a length of 5 mm and a diameter of 4.7 mm, the maximum stress was observed at the junction of the implant abutment when the implant was placed at an angle of 30° and the models used a vertical force, and the minimum stress occurred in the apical 1/3 region of the implant. The maximum stress occurred between the implant and the abutment when the implant was placed at an angle of 30° and the models applied a force in the oblique direction, and minimal stress occurred at the apical region. According to the stress analysis obtained from

implants with a length of 10 mm and a diameter of 3.7 mm, the maximum stress occurred just below the neck of the implant when the implant was placed at a right angle and the models used a vertical force, and the minimum stress occurred in the apical 1/3 region of the implant. The maximum stress occurred in the neck of the implant when the implant was placed at a right angle and the models applied a force in the oblique direction, and the minimum stress occurred in the apical 1/3 region of the implant. The maximum von misses stress was seen at the junction of the implant abutment when the implant was placed at an angle of 30° and the models used a vertical force, and the minimum stress occurred at the apical region of the implant. The maximum stress occurred between the implant and the abutment when the implant was placed at an angle of 30° and the models applied a force in the oblique direction and minimal stress occurred at the apical region.

According to the stress analysis obtained from the implants with a length of 10 mm and a diameter of 4.7 mm, the maximum stress occurred in the neck of the implant when the implant was placed at a right angle and the models used a vertical force, and the minimum stress occurred in the apical 1/3 region of the implant. The maximum stress occurred in the neck of the implant when the implant was placed at a right angle and the models applied a force in the oblique direction, and the minimum stress occurred in the apical 1/3 region of the implant. The maximum stress was observed in the neck of the implant when the implant was placed at an angle of 30° and the models used a vertical force, and the minimum stress occurred in the apical 1/3 region of the implant. The maximum stress occurred between the implant and the abutment when the implant was placed at an angle of 30° and the models applied a force in the oblique direction, and the minimum stress occurred in the apical 1/3 region of the implant.

According to the stress analysis obtained from the implants with a length of 13 mm and a diameter of 3.7 mm, the maximum stress occurred in the neck of the implant when the implant was placed at a right angle and the models used a vertical force, and the minimum stress occurred at the apical region of the implant. The maximum stress occurred in the neck of the implant when the implant was placed at a right angle and the models applied a force in the

oblique direction, and the minimum stress occurred in the apical 1/2 region of the implant. The maximum stress was observed in the neck of the implant when the implant was placed at an angle of 30° and the models used a vertical force, and the minimum stress occurred at the apical region of the implant. The maximum stress occurred between the implant and the abutment when the implant was placed at an angle of 30° and the models applied a force in the oblique direction, and minimal stress occurred at the apical region of the implant.

According to the stress analysis obtained from the 13 mm long and 4.7 mm in diameter implants, the maximum stress occurred in the neck of the implant when the implant was placed at a right angle and the models used a vertical force, and the minimum stress occurred at the apical region of the implant. The maximum stress occurred in the neck of the implant when the implant was placed at a right angle and the models applied a force in the oblique direction, and the minimum stress occurred in the apical 1/2 region of the implant. The maximum stress was observed in the neck of the implant when the implant was placed at an angle of 30° and the models used a vertical force, and the minimum stress occurred in the apical 1/3 region of the implant. The maximum stress occurred between the implant and the abutment when the implant was placed at an angle of 30° and the models applied a force in the oblique direction, and minimal stress occurred at the apical region of the implant.

Statistical analysis

In this study, the stress caused by endosteal implants with different diameters and lengths placed in the maxilla and mandible was compared using the 3D finite element stress analysis method. Since the numerical values obtained with the mathematical models used in the study were constant and had no variance, a statistical analysis was not performed to evaluate the findings.

Discussion

Many finite element stress analysis studies have been conducted to examine the stress distribution in the bones surrounding implants.^{17,18} Recently, two-dimensional (2D) and 3D finite element stress analyses have been performed to investigate how prostheses

supported by implants affect the stress distribution in bones.¹⁹ Therefore, with the possibilities and conveniences of today's technology, our working models are prepared in detail and meticulously in 3D in accordance with the real anatomy.

Many studies have been conducted on implant material, implant design, superstructure material, implant-crown ratio, and the implant bone interface mechanism, which are the factors that affect stress distribution.^{20,21} The stress distributions that occur in implants are also widely used in tensile meters and photoelastic methods as well as the finite element stress analysis method. Clelland et al. stated that although the photoelastic method provided qualitative information about the stress concentration and location, it provided limited quantitative data.²²

It has been emphasized that finite element stress analysis provides any detailed quantitative feeder on a mathematical model.²² In this stress analysis method, although 3D studies can be performed on the bone using the photoelastic method, it is not preferred, because it is difficult to reduce the size of the implant model originals and the stress at the depth cannot be reached in the tension meter. For this reason, the finite element stress analysis method, which is preferred by many researchers, was used in our study.

Bone modeling has been done in a variety of ways in the literature. For example, Wang et al. used a 42 mm long, 11 mm wide, and 21 mm high bone block and determined the cortical bone thickness as 2 mm.²³ In another study, a bone block with a height of 23.4 mm, a width of 12.8 mm, and a thickness of 9 mm and cortical bone of 1.3 mm thickness were modeled.²⁴ In our study, maxilla and mandible models of 30 mm x 20 mm x 10 mm were obtained.

In 2014, Ciccio et al. conducted another finite element stress analysis study and analyzed the masticatory forces of implants with 4 different designs. They reported that changing the implant neck geometry caused resorption in the alveolar bone due to the increase in stress in the implant neck region.²⁵ Furthermore, Tao Li et al. applied the finite element stress analysis technique in a study they conducted in 2011 to detect the most ideal diameter and size implant in the posterior mandible. As a result of this study, it was determined that the primary stability in the posterior mandible increased with the increase in

the diameter of the implant. It has also been shown that increasing the diameter of the implant in the posterior mandible reduces the stress on the neck of the implant. Another result obtained is that the optimum implant is 4.0 mm in diameter and 12 mm in length.⁴ In addition, according to the results of the stress analysis conducted by El-Anwar et al. on implant design in 2011, the increase in the length or diameter of the implant did not significantly change the stress values in the neck region of the implant.²⁶ However, in the study conducted by Santiago et al. in 2013, increasing the implant diameter with oblique forces caused less resorption in the bone. In addition, they reported that oblique forces caused more resorption in bone compared to vertical forces.²⁷ In yet another study conducted by Giuseppe et al. in 2013, the effect of the thread shape, diameter, and length of the implant on stress was compared. The change in the implant diameter is more significant than the change in implant length and thread shape. In other words, as the diameter of the implant increases, the stress in the neck area will decrease. In this respect, similar results were obtained in our study.²⁸ Moreover, in 2019, Yalcin et al. concluded that increasing the implant length is not enough to reduce the stress distribution in the neck area of the implant. In other words, by increasing the implant length, the stress in the neck area of the bone has not been sufficiently reduced. This is a result parallel to our study. In addition, it has been emphasized that not choosing the correct thread design of the implant is the most effective parameter in the failure of the implant.²⁹ Guven et al., in 2015, reported that the stress values in an angled implant are higher than in an implant placed vertically. This means that implants placed at an angle cause more stress in the neck area. This supports the data we obtained in our study.³⁰ Furthermore, in a study conducted by Wang et al. in 2016, the change of the implant angle in the model bone revealed that the implant affects the amount and distribution of stress in the neck region and alveolar bone.³¹

According to our results, the stress values in the maxilla reached higher values than the mandible. There are many implant companies in the market now, and the dental implants produced by these companies have very different diameters and lengths. In our study, a stress analysis was performed by selecting implants of

different lengths and diameters. When modeling the implant diameter, an implant diameter (3.7 mm and 4.7 mm) close to the average diameter of the most commonly used implant brands was preferred. The implant length was modeled in three dimensions by selecting 5 mm, 10 mm and 13 mm. We observed that the stresses in the implants with a diameter of 3.7 mm were greater than in implants of the same size but with a diameter of 4.7 mm.

Conclusions

Taken together, in all models, under each loading condition, as the implant diameter and length increased, the stress levels in the bone and implant decreased. Thus, implant diameter is more effective than implant length at changing the stress values. There was a significant increase in the stress levels of the cortical bone and implants in the oblique loading models compared to the vertical loading models. In 3D models with cortical bone, the highest stress values in the bone were detected in the parts (neck region) where the implant first touches the cortical bone. For the angled implants, there was less stress accumulation in the implant in the 3D models where the force was applied vertically compared to the models where the force was applied obliquely. Thus, we concluded that thin-diameter implants cause more stress on oblique placement and loading than thick-diameter implants. However, additional studies are needed for more accurate results.

Acknowledgements

This article reports a part of the PhD dissertation written by the first author and supervised by the second author. The dissertation was supported by DUBAP with the project number 12- DH-76.

Declaration of Interest

The authors report no conflict of interest.

References

1. Jinmeng L, John AJ, Frank W, Jeroen JJP. Mechanical aspects of dental implants and osseointegration: A narrative review. *Journal of mechanical behavior of biomedical materials*. 2020; 103(3): 1-11.
2. Cervino G, Romeo U, Lauritano F, Bramanti E, Fiorillo L, D'Amico C, Milone D, Laino L, Campolongo F, Rapisarda S, Cicciù M. Fem and Von Mises Analysis of OSSTEM® Dental Implant Structural Components: Evaluation of Different Direction Dynamic Loads. *The Open Dentistry Journal*. 2018; 30(12): 219-229.

3. Chun HJ, Cheong SY, Han JH, Heo SJ, Chung JP, Rhyu IC, Choi YC, Baik HK, Ku Y, Kim MH. Evaluation of design parameters of osseointegrated dental implants using finite element analysis. *Journal of Oral Rehabilitation*. 2002; 29(6): 565-74.
4. Li T, Hu, K, Cheng L, Ding Y, Shao J, Kong L. Optimum selection of dental implant diameter and length in the posterior mandible with poor bone quality: A 3D finite element analysis. *Applied Mathematical Modelling*. 2011; 35(1): 446-456.
5. Sevımay M, Turhan F, Kılıçarslan MA, Eskitaşçıoğlu G. Three dimensional finite element analysis of the effect of different bone quality on stress distribution in an implant-supported crown. *Journal of Prosthetic Dentistry*. 2005; 93(3): 227-234.
6. Şahin S, Çehreli MC, Yalçın E. The influence of functional forces on the biomechanics of implant-supported prostheses- A review. *Journal of Dentistry*. 2002; 30(7- 8): 271-282.
7. Tonetti MS. Determination of the success and failure of root-form osseointegrated dental implants. *Advances in Dental Research*. 1999; 13(1): 173-180.
8. Bidez MW, Misch CE. Force transfer in implant dentistry: basic concepts and principles. *Journal of Oral Implantology*. 1992; 18(3): 264-274.
9. Van Staden RC, Guan H, Loo YC. Application of the finite element method in dental implant research. *Computer Methods in Biomechanics and Biomedical Engineering*. 2006; 9(4): 257-270.
10. Geng JP, Tan KB, Liu GR. Application of finite element analysis in implant dentistry: a review of the literature. *Journal of Prosthetic Dentistry*. 2001; 85(6): 585-598.
11. Weinstein AM, Klawitter JJ, Anand SC, Schuessler R. Stress analysis of porous rooted dental implants. *Journal of Dental Research*. 1976; 55(5): 772-777.
12. DeTolla DH, Andreana S, Patra A, Buhite R, Comella B. The role of the finite element model in dental implants. *Journal of Oral Implantology*. 2000; 26(2): 77-81.
13. Bathe KJ, Zhang H, Wang MH. Finite element analysis of incompressible and compressible fluid flows with free surfaces and structural interactions. *Computers and Structures*. 1995; 56(2): 193-213.
14. Bozkaya D, Müftü S, Müftü A. Evaluation of load transfer characteristics of five different implants in compact bone at different load levels by finite elements analysis. *Journal of Prosthetic Dentistry*. 2004; 92(6): 523-530.
15. Ulm C, Kneissel M, Schedle A, Solar P, Matejka M, Schneider B, Donath K. Characteristic features of trabecular bone in edentulous maxillae. *Clinical Oral Implants Research*. 1999; 10(6): 459-467.
16. Clelland NL, Gilat A. The effect of abutment angulation on stress transfer for an implant. *Journal of Prosthodontics*. 1992; 1(1): 24-28.
17. Tepper G, Haas R, Zechner W, Krach W, Watzek G. Three-dimensional finite element analysis of implant stability in the atrophic posterior maxilla: a mathematical study of the sinus floor augmentation. *Clinical Oral Implants Research*. 2002; 13(6): 657-65.
18. Koca OL, Eskitascioglu G, Usumez A. Three-dimensional finite-element analysis of functional stresses in different bone locations produced by implants placed in the maxillary posterior region of the sinus floor. *Journal of Prosthetic Dentistry*. 2005; 93(1): 38-44.
19. Ismail YH, Pahountis LN, Fleming JF. Comparison of two-dimensional and three-dimensional finite element analysis of a blade implant. *International Journal of Oral Implantology*. 1987; 4(2): 25-31.
20. Hansson S, Werke M. The implant thread as a retention element in cortical bone: the effect of thread size and thread profile: a finite element study. *Journal of Biomechanics*. 2003; 36(9): 1247-58.
21. Hedia HS. Effect of coating thickness and its material on the stress distribution for dental implants. *Journal of Medical Engineering Technology*. 2007; 31(4): 280-7.
22. Clelland NL, Lee JK, Bimbenet OC, Brantley WA. A three-dimensional finite element stress analysis of angled abutments for an implant placed in the anterior maxilla. *Journal of Prosthodontics*. 1995; 4(2): 95-100.
23. Wang TM, Leu LJ, Wang J, Lin LD. Effects of prosthesis materials and prosthesis splinting on peri-implant bone stress around implants in poor-quality bone: a numeric analysis. *The International Journal of Oral & Maxillofacial Implants*. 2002; 17(2): 231-7.
24. Tada S, Stegaroiu R, Kitamura E, Miyakawa O, Kusakari H. Influence of implant design and bone quality on stress/strain distribution in bone around implants: A 3-dimensional finite element analysis. *International Journal Oral & Maxillofacial Implants*. 2003; 18(3): 357-368.
25. M. Ciccio, E. Bramanti, F. Cecchetti, L. Scappaticci, E. Gugliel, G. Risitano. FEM and Von Mises analyses of different dental implant shapes for masticatory loading distribution. *Oral & Implantology*. 2014; 7(1): 1-10.
26. El-Anwar MI, El-Zawahry MM. A three dimensional finite element study on dental implant design. *Journal of Genetic Engineering Biotechnology*. 2011; 9(1): 77-82.
27. Santiago JF, Pellizzer EP, Verri FR. Stress analysis in bone tissue around single implants with different diameters and veneering materials: A 3-D finite element study. *Material Science and Engineering: C*. 2013; 33(8): 4700-14.
28. Vairo G, Sannino G. Comparative evaluation of osseointegrated dental implants based on platform-switching concept: Influence of diameter, length, thread shape, and in-bone positioning depth on stress-based performance. *Computational and Mathematical Methods in Medicine*. 2013; Article ID 250929, 15 pages 1-15.
29. Yalcin M, Kaya B, Lacin N, Ari E. Three-Dimensional Finite Element Analysis of the Effect of Endosteal Implants with Different Macro Designs on Stress Distribution in Different Bone Qualities. *International Journal Oral & Maxillofacial Implants*. 2019; 34(3): 43-50.
30. Guven S, Atalay Y, Asutay F, Ucan MC, Dunder S, Karaman T, Gunes N. Comparison of the effects of different loading locations on stresses transferred to straight and angled implant-supported zirconia frameworks: a finite element method study. *Biotechnology and Biotechnological Equipment*. 2015; 29(4): 684-690.
31. Wang C, Zhang W, Ajmera DH, Zhang Y, Fan Y, Ji P. Simulated bone remodeling around tilted dental implants in the anterior maxilla. *Biomechanical Model Mechanobiol*. 2016; 15(1): 701-712.